

Wire array experiments in a low impedance and low current generator

This content has been downloaded from IOPscience. Please scroll down to see the full text.

2015 J. Phys.: Conf. Ser. 591 012026

(<http://iopscience.iop.org/1742-6596/591/1/012026>)

View [the table of contents for this issue](#), or go to the [journal homepage](#) for more

Download details:

IP Address: 146.155.28.40

This content was downloaded on 17/05/2016 at 22:49

Please note that [terms and conditions apply](#).

Wire array experiments in a low impedance and low current generator

Nibaldo Cabrini³, Cristian Pavez^{1,2,3}, Gonzalo Avaria^{1,2}, Patricio San Martín^{1,2}, Felipe Veloso⁵, Barbara Zúñiga⁴, Adolfo Sepúlveda⁴, and Leopoldo Soto^{1,2,3}

¹Comisión Chilena de Energía Nuclear – Chile

²Center for Research and Applications in Plasma Physics and Pulsed Power – P4 Chile

³Departamento de Ciencias Físicas, Universidad Andrés Bello, Chile

⁴Facultad de Ingeniería, Universidad Mayor, Santiago, Chile

⁵Instituto de Física, Pontificia Universidad Católica de Chile, Santiago, Chile

E-mail: cpavez@cchen.cl

Abstract. In this work, a preliminary study about the behavior of a low impedance generator on different wire array configurations is reported. The experimental measurements were carried out on a small multi-purpose generator (1.2 μ F, 345J, 47.5nH, T/4=375 ns and Z=0.2 Ω in short circuit) which produces currents up to 122 kA with 500 ns quarter period, when a charging voltage of 24kV and a wire load are used. Two types of configurations were tested: parallel wires (two and four) and X-pinch configurations. The experiments were carried out on W, Al, and Cu wires with different diameters. The discharge was characterized by means of a set of diagnostics which included: Rogowski coil; filtered PCD detector; filtered PIN diode; gated VUV/soft X-ray pinhole camera, Shadow diagnostic and dark field Schlieren technique. From the set of experimental results, the following observations can be established: (i) The generator is highly sensitive to the changes of load impedance due to its low impedance design. (ii) Every shot shows a dip in the current derivative signal shortly after the discharge onset time (from 6 to 40 ns), which is inversely related to the load resistance. (iii) Both configurations show a similar dynamic to those observed in experiments of higher current and shorter quarter period. (iv) At the X-pinch experiments, two or more hard X-ray bursts are detected, around 200 ns from the current onset time. These X-ray bursts are correlated with the dips observed in the current derivative signal.

1. Introduction

Nowadays is widely known that the Z-pinches are the most powerful X-ray radiation source produced at the laboratories, particularly those configurations based on wire array [1]. Of these, two types capture the attention by the characteristics of the emission source: the cylindrical wire array and the X-pinch configurations. In the first, several metallic wires cylindrically arranged connect the electrodes. In the X-pinch configuration, two diagonal wires are assembled between the electrodes, touching only at the cross point, forming an "X". In both configurations, either the skin-depth effect or the low inductance path favors a current flow in the wire surface. This current flow ablates mass by Joule effect creating a hot, low-density coronal plasma that surround a cold and dense structure. On this coronal plasma flows the bulk of the current. The subsequent dynamic is governed by the characteristics of the precursor plasma and its interaction with the global magnetic field. In the wire



array experiments, the migration of the precursor plasma to the symmetry axis is accompanied in the final phase of the discharge by a violent collapse of the residual plasma on the discharge axis. In the stagnation, the thermalized hot plasma produces intense soft X-ray pulses, which have been used in the Z-machine to produce inertial confinement fusion [1, 2]. At the X-pinch configuration a significant effect of the global magnetic field is obtained in the cross point, where a hot, dense micro-pinch is originated. In these conditions, the plasma yields an intense and small soft X-ray source of short duration, ideal for applications. At the Cornell University facilities, X-pinch experiments driven in a large generator, size sources of less than $1\mu\text{m}$ and time-durations of less than 1ns have been reported [3]. In all experiments of wire arrays Z-pinch above mentioned, the experiments are driven in expensive and complex generators, characterized by high peak currents and current rates faster than 1kA/ns .

The interest for intense and short duration X-ray pulses has been extended to wire array experiments of lower power, whose rise times are between 200 ns - 800 ns [4, 5]. In this direction, a new generation of X-pinch is being developed with lower energy generators and current rise-rates lower than 1kA/ns (low-current and long-time), as those driven in capacitive storage systems [6-8], or in a compact device based in transmission line for applications [9-12]. Motivated by recent developments, we decided to study the behavior of a low impedance capacitive generator [13], in the range of low currents ($\sim 120\text{kA}$), using metallic wire arrays in two configurations: two and four parallel wire configuration and X-pinch configuration. In both, a wide variety of different diagnostics was used.

2. Experimental setup

2.1 The Multipurpose generator

The experiments reported here were carried out on a compact capacitive generator (Multipurpose generator) made at the Chilean Nuclear Energy Commission (CCHEN). These experiments correspond to the first time the generator operated with a plasma load. The generator consist of a capacitive bank formed by four capacitors of $0.3\mu\text{F}$ connected in parallel, a triggerable switch (spark-gap) and a discharge chamber with nine windows for diagnostics and vacuum system. Figure 1 show a picture of the generator assembled on a surface of $1.1\times 1.1\text{m}^2$, with the discharge chamber at the center. For the wire array experiments, compact electrode configuration and isolation systems were built. The assembly of electrodes is shown in Figure 1b. A summary of electrical parameters of the generator are listed in Table 1. The generator inductance with the electrodes corresponds to the minimum value in order to see the wire array through the chamber windows.

2.2 Diagnostics

In order to define the scope of the wire array experiments using the multipurpose generator, an ample set of diagnostics were mounted, both time-resolved and time integrated. Of the first type, a Rogowski coil; filtered PCD detector; filtered PIN diode; gated VUV/soft X-ray pinhole camera, Shadow diagnostic and dark field Schlieren diagnostic were used. To image the plasma for photon energies higher than 3keV , a time-integrated filtered pinhole system was implemented. On the other hand, the series of experiments developed here produced the ideal environment, which allowed us to test many of the above mentioned diagnostics.

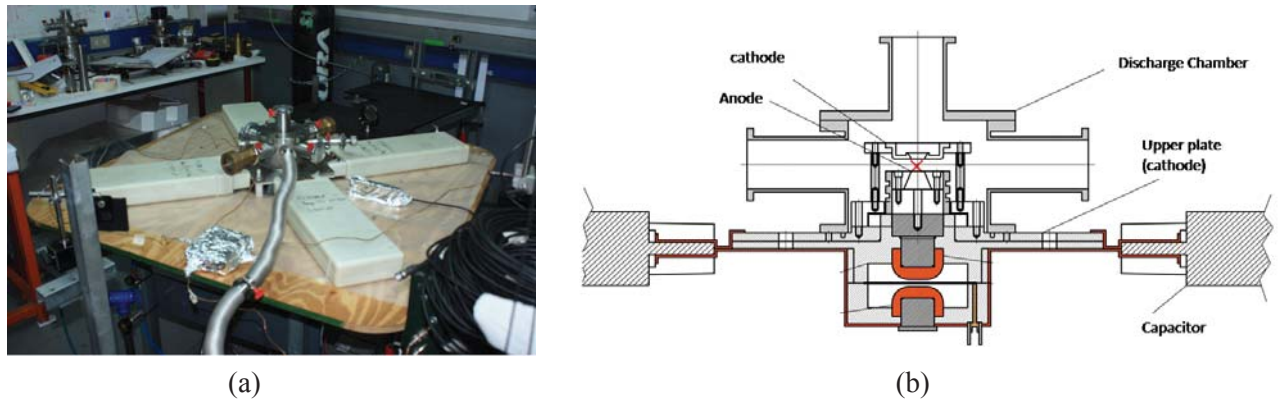


Figure 1. (a) Panoramic view of generator, (b) Cross section the generator and electrode configuration.

Table 1. Electrical parameters of the generator.

	$C(\mu F)$	$L(nH)$	$V_{max}(kV)$	$E_{load}(J)$	$I_{peak}(kA)$	$T/4(ns)$	$Z(\Omega)$
Short circuit without electrodes	1.2	33	30	540	180	313	0.17
Short circuit with electrodes	1.2	47.5	30	540	150	375	0.2

2.3 Used wire array configurations

Figure 2 depicts the wire assemblies for each configuration. The side-on view gives account the effective spacing between wires that the imaging system records. Both the electron gap and the wire array diameter are 1cm.

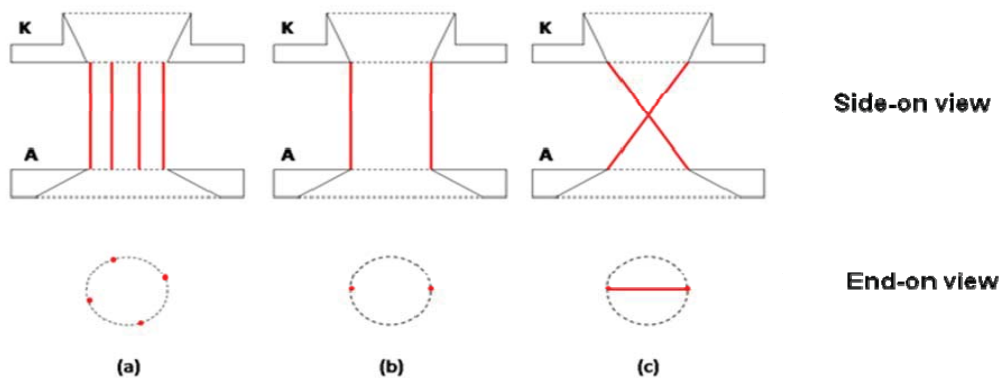


Figure 2. Schematic representation of the assembly of wire array.

3. Experimental results

3.1 Parallel wire array. General behavior

From figure 3, it is possible to recognize the three typical phases observed in wire array experiments of higher current and rise rate. (a) Modulation of the plasma density along the axis. Appearance of coronal plasma and instabilities. (b) Ablation and precursor plasma migration. (c) Plasma column formation (stagnation). The pictures correspond to pin-hole images recorded on a VUV-MCP camera with an exposure time of 4ns. In wire array experiments x-rays were not detected either on the PIN diode or on the PCD detector.

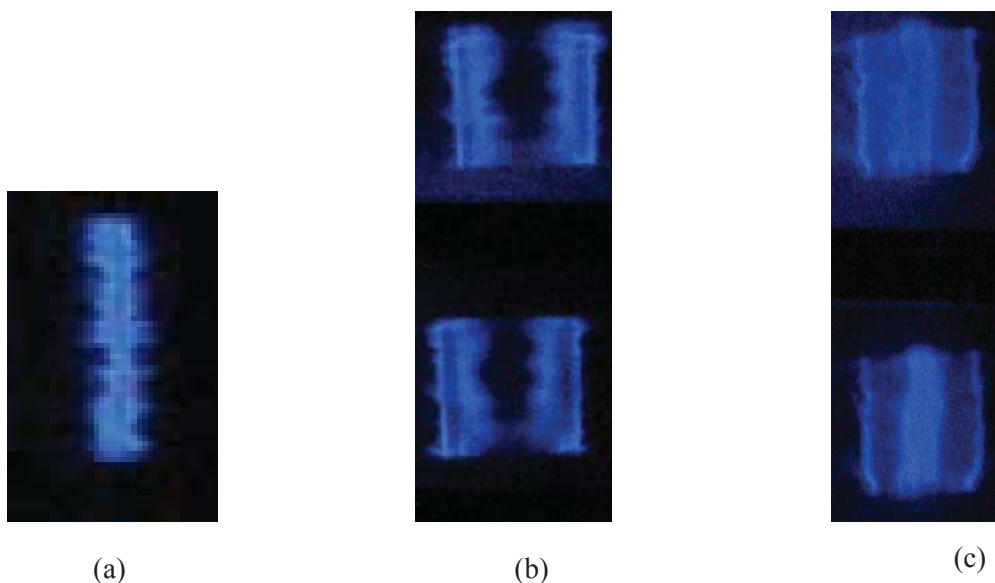


Figure 3. Formation and dynamics of plasma. (b) and (c) correspond to two aluminum wire of $50 \mu\text{m}$.

3.2 X-pinch

In this subsection we report the main characteristics observed on the X-pinch discharge by means of the diagnostics above mentioned. In this configuration all radiation diagnostics recorded X-rays (from soft-X-ray to harder radiation): both the filtered PIN diode and the PCD detector detected X-rays since the beginning of the fast compression of the micro-pinch until the subsequent rupture. Figure 4 shows the structure and dynamics of the X-pinch on different systems of image recording. Figure 4(a) shows a sequence of pin-hole images in the VUV spectral range. Figure 4(b) and 4(c) show a Shadow and Schlieren record respectively, for which it was used a Nd:YAG power laser at 532 nm and 8-ns pulsewidth.. In each diagnostics the time is taken with respect to the discharge onset time.

Figure 5 shows a set of electrical signals for a typical shot on Tungsten X-pinch (W of $7.5 \mu\text{m}$). In this shot, multiple singularities (dip) appear in the current derivative signal (about 50 kA and 75 kA) thus, the current signal shows a decrease in the rise rate of current, followed by multiple bursts of X-rays. This is evident from the consecutive peaks observed in both the PCD detector and PIN diode.

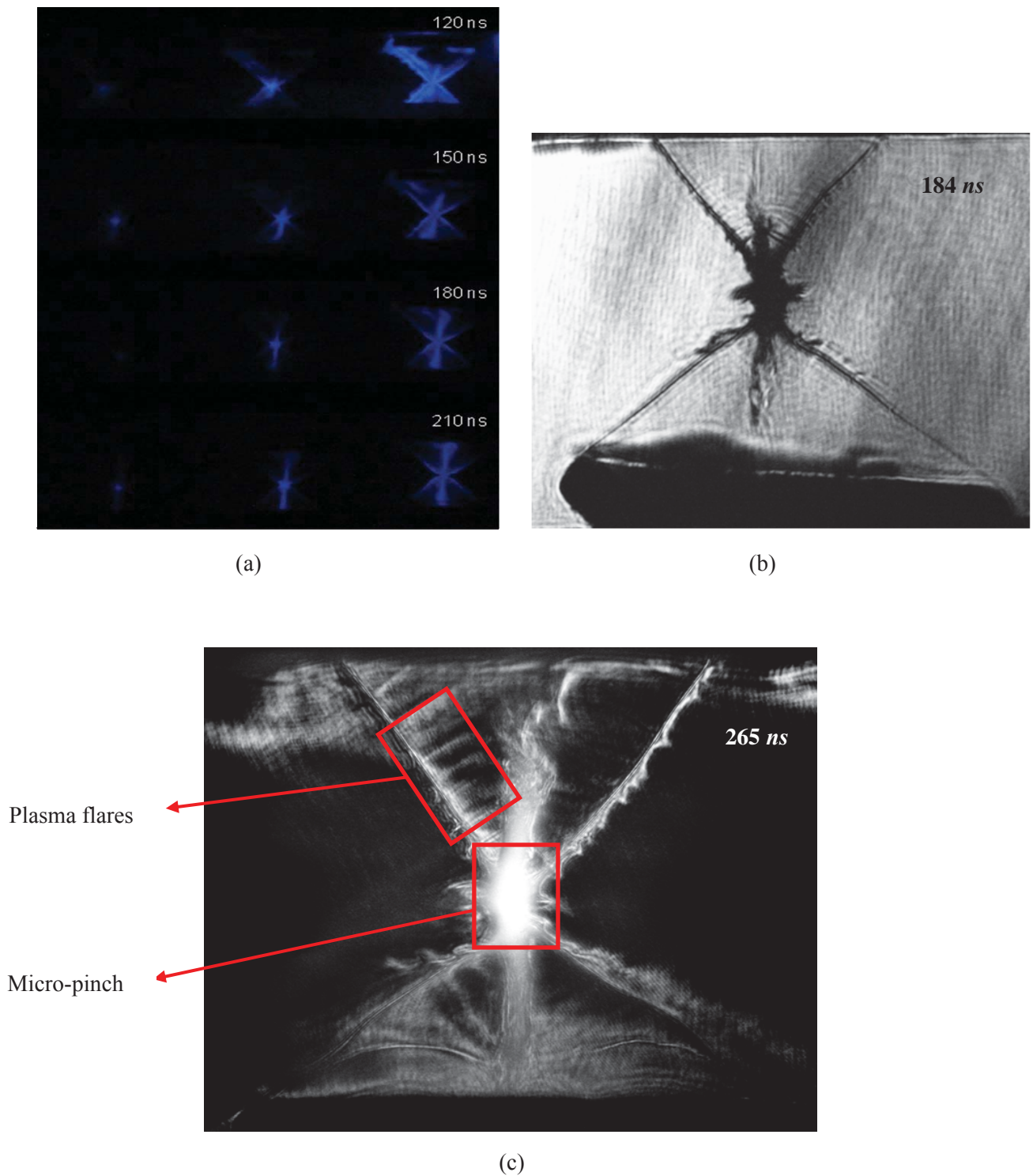


Figure 4. (a) VUV pinhole image of aluminum X-pinch of 25 μm . (b) Image-plane Shadowgraph of Tungsten X-pinch of 13 μm . (c) Dark field Schlieren of Tungsten X-pinch of 13 μm

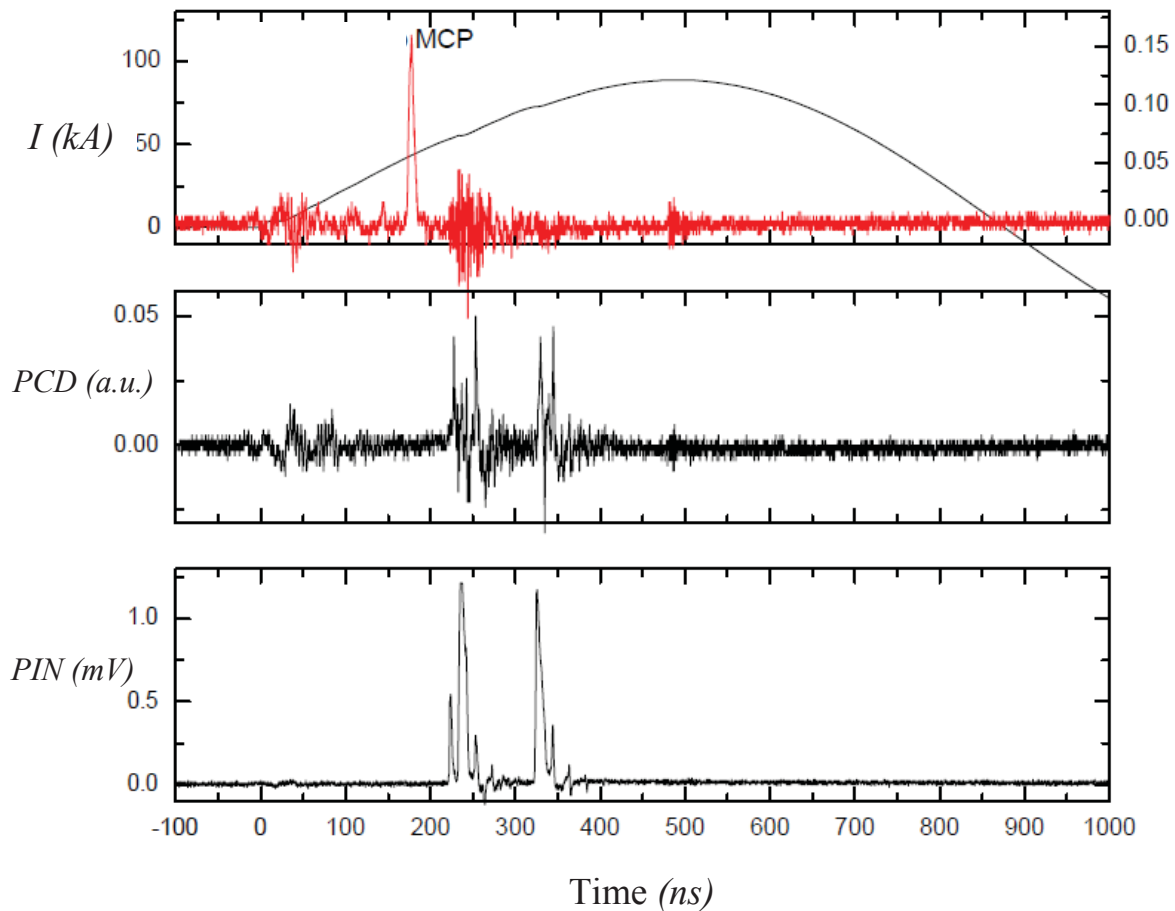


Figure 5: Electrical signals for a typical shot on Tungsten X-pinch (W of 7.5 μm).

3.2 Initial load behavior

In this subsection, we report the electrical behavior observed in the current derivative signals (I_{dot}) shortly after the discharge onset time (from 6 to 40 ns). In all wire array signals a dip was observed whose onset time is inversely related with the initial resistance of the wire array. Here, we calculate the initial resistance by means of the relation $R = \rho L/A$, where ρ is the resistivity of the material, L the length of the wire and A the cross section area. This reproducible behavior could be giving account of the solid-liquid-vapour transition in the wire, dominated by an increase of the resistivity, which is easily detected for a low impedance generator as the Multipurpose generator. The relation between the load resistance and the dip onset time is shown in Fig. 6.

3.2 Applications

In order to illustrate the potentiality of the X-ray sources based in X-pinch, furthermore to make a complementary qualitative diagnostic, an insect radiograph was made. The X-pinch was made of Tungsten of 7.5 μm and the radiography was recorded on a dental film filtered with an Al foil of 15 μm , without the original packaging. The radiography is shown in Fig. 7.

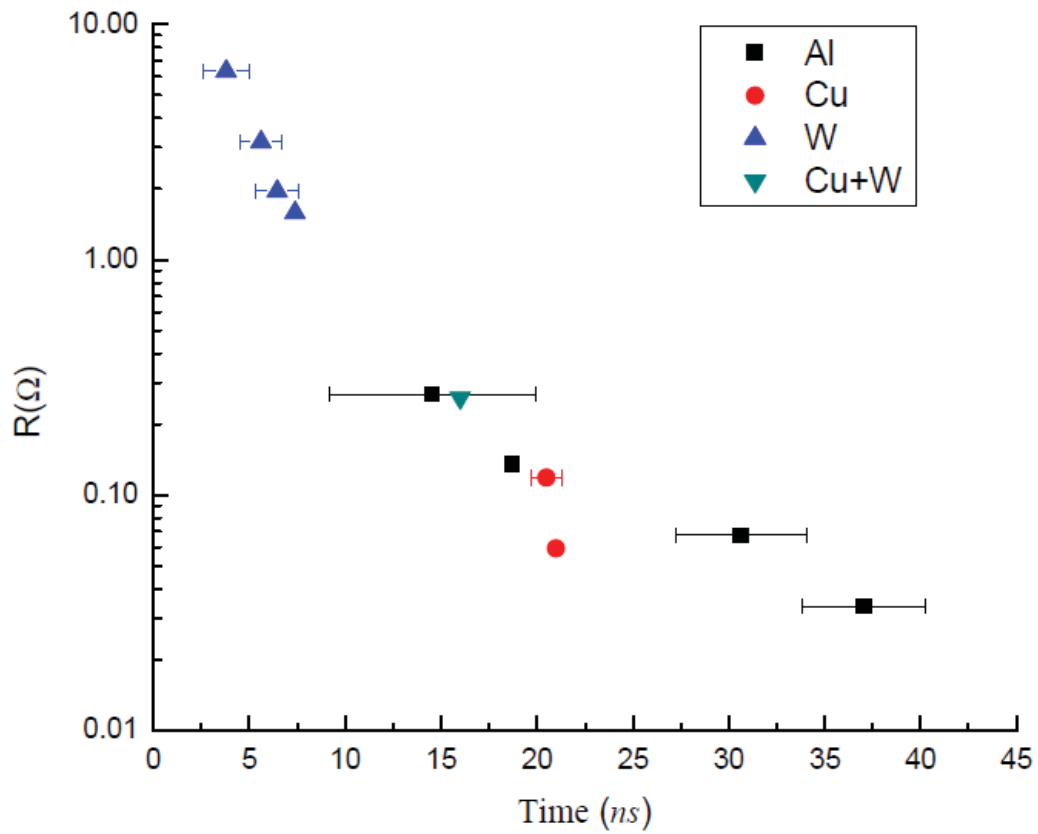


Figure 6: Experimental relation between the wire array resistance and the dip onset time.



Figure 7: Insect radiography using Tungsten X-pinch of 7.5 μm.

4. Remarks and conclusion

From the set of diagnostics and experimental results, a first approach to the dynamic and emission of the plasma, under wire array experiments can be summarized as following:

- The generator is highly sensitive to the changes of load impedance due to its low design impedance.
- Experiments with metallic wire conducted on the multipurpose generator showed similar characteristics to those observed in higher currents and high current rate generators ($\geq 10^{12}$ A/s), namely: density modulation along the wire and migration of precursor plasma because of the global magnetic field (similar dynamics).
- Every shot shows a dip in the current derivative signal shortly after the discharge onset time (from 6 to 40 ns), which is inversely related to the load resistance.
- In wire array experiments, a central plasma column at the final stage of the ablation is observed. For X-pinch experiments, a plasma jet and a micro-pinch with high emission of X-ray were observed in the crossing point of the wires.
- Up to now, there is no experimental evidence that a significant X-ray production is taking place. The presence of soft X-ray gives account of a high temperature plasma, which is observed in the micro-pinch region (crossing point).
- Two or more hard X-ray bursts were detected around 200 ns from the current onset time. These X-ray bursts are correlated with the dips observed in the current derivative signal.
- From the refractive optical diagnostics, the x-pinch dynamic is similar to that observed in other x-pinch experiments, characterized by the formation of plasma flares feeding a plasma jet in the axis of symmetry of the discharge in addition to the formation of a bright micro-pinch in the cross point.

New experiments are being developed in order to quantify and characterize each observation here described.

The authors would like to acknowledge financial support by PIA CONICYT grant ACT 1115. G. Avaria acknowledges the financial support from PAI CONICYT 791100020 and FONDECYT Iniciación 11121587.

References

- [1] M. Haines, "A review of the dense Z-pinch", *Plasma Phys. Control. Fusion* **53** (2011).
- [2] C. L. Ruiz, G. W. Cooper, S. A. Slutz, J. E. Bailey, G. A. Chandler, T. J. Nash, T. A. Mehlhorn, R. J. Leeper, D. Fehl, A. J. Nelson, J. Franklin, and L. Ziegler. *Phys. Rev. Lett.* Vol. **93**, 1 (2004).
- [3] S. A. Pikuz, et al, "High energy density z-pinch plasma conditions with picosecond time resolution". *Phys. Rev. Lett.*, **89**, 035003 (2002).
- [4] C. Deeney, C. A. Coverdale, and M. R. Douglas, *Laser and Particle Beams*, **19**, 497-506, (2001).
- [5] H. Calamy, F. Hamann, F. Lassalle, J. Chittenden, S. V. Lebedev, F. Bayol, Ch. Mangeant, A. Morell, D. Huet, and J-P. Bedoch, *IEEE Trans. Plas.Sci.*, **34**, 2279 (2006).
- [6] Christou C, Dangor A E and Hammer D A 2000 *J Appl Phys* **87** 8295-8303.
- [7] Aranchuk L E, Chuvatin A S and Larour J 2004 *Rev Sci Instrum* **75** 69-74.
- [8] Aranchuk L E, Larour J and Chuvatin A S 2005 *IEEE Trans Plasma Sci* **33** 990-996.
- [9] G. W. Collins IV, Ms. Of Science in physic, "Study of X-pinch dynamics using a low current

- (25kA) and long-rising (400ns) pulse". San Diego State University, 2013.
- [10] G. W. Collins IV, et al "Study of X-pinch dynamics using a low current (25kA) and slower current (400ns) pulse". *Phys. Plasmas*. **20**, (2013).
 - [11] G. W. Collins IV, et al "Effect of the global to local magnetic field ratio on the ablation modulations on X-pinches driven by 80kA peak current". *New Journal of Physics*. **14**, (2012).
 - [12] D. M. Haas, et al "Supersonic jet formation and propagation in X-pinches". *Astrophys. Space Sci* (2013) 336: 33-40.
 - [13] A. Tarifeño, C. Pavez, M. Cardenas, L. Soto, *Phys. Scr.* **T131** (2008) 014028 (5pp).